

---

# CRoSS: Diffusion Model Makes Controllable, Robust and Secure Image Steganography

---

Anonymous Author(s)

## Abstract

1 Current image steganography techniques are mainly focused on cover-based meth-  
2 ods, which commonly have the risk of leaking secret images and poor robustness  
3 against degraded container images. Inspired by recent developments in diffu-  
4 sion models, we discovered that two properties of diffusion models, the ability to  
5 achieve translation between two images without training, and robustness to noisy  
6 data, can be used to improve security and natural robustness in image steganogra-  
7 phy tasks. For the choice of diffusion model, we selected Stable Diffusion, a type  
8 of conditional diffusion model, and fully utilized the latest tools from open-source  
9 communities, such as LoRAs and ControlNets, to improve the controllability and  
10 diversity of container images. In summary, we propose a novel image steganogra-  
11 phy framework, named Controllable, **R**obust and **S**ecure Image Steganography  
12 (CRoSS), which has significant advantages in controllability, robustness, and secu-  
13 rity compared to cover-based image steganography methods. These benefits are  
14 obtained without additional training. To our knowledge, this is the first work to  
15 introduce diffusion models to the field of image steganography. In the experimental  
16 section, we conducted detailed experiments to demonstrate the advantages of our  
17 proposed CRoSS framework in controllability, robustness, and security.<sup>1</sup>

## 18 1 Introduction

19 With the explosive development of digital communication and AIGC (AI-generated content), the  
20 privacy, security, and protection of data have aroused significant concerns. As a widely studied  
21 technique, steganography [10] aims to hide messages like audio, image, and text into the container  
22 image in an undetected manner. In its reveal process, it is only possible for the receivers with pre-  
23 defined revealing operations to reconstruct secret information from the container image. It has a wide  
24 range of applications, such as copyright protection [4], digital watermarking [13], e-commerce [11],  
25 anti-visual detection [32], and cloud computing [74].

26 For image steganography, traditional methods tend to transform the secret messages in the spatial  
27 or adaptive domains [25], such as fewer significant bits [9] or indistinguishable parts. With the  
28 development of deep neural networks, researchers begin to use auto-encoder networks [5, 6] or  
29 invertible neural networks (INN) [33, 24] to hide data, namely deep steganography.

30 The essential targets of image steganography are security, reconstruction quality, and robustness [9,  
31 43, 75]. Since most previous methods use cover images to hide secret images, they tend to explicitly  
32 retain some secret information as artifacts or local details in the container image, which poses a risk  
33 of information leakage and reduces the **security** of transmission. Meanwhile, although previous  
34 works can maintain well reconstruction fidelity of the revealed images, they tend to train models in a  
35 noise-free simulation environment and can not withstand noise, compression artifacts, and non-linear  
36 transformations in practice, which severely hampers their practical values and **robustness** [28, 42, 23].

37 To address security and robustness concerns, researchers have shifted their focus toward coverless  
38 steganography. This approach aims to create a container image that bears no relation to the secret  
39 information, thereby enhancing its security. Current coverless steganography methods frequently

---

<sup>1</sup>For reproducible research, the complete source codes of our method will be made publicly available.

40 employ frameworks such as CycleGAN [76] and encoder-decoder models [74], leveraging the  
41 principle of cycle consistency. However, the **controllability** of the container images generated by  
42 existing coverless methods remains limited. Their container images are only randomly sampled from  
43 the generative model and cannot be determined by the user. Moreover, existing approaches [45] tend  
44 to only involve hiding bits into container images, ignoring the more complex hiding of secret images.  
45 Overall, current methods, whether cover-based or coverless, have not been able to achieve good unity  
46 in terms of security, controllability, and robustness. Thus, our focus is to propose a new framework  
47 that can simultaneously improve existing methods in these three aspects.

48 Recently, research on diffusion-based generative models [20, 53, 54] has been very popular, with  
49 various unique properties such as the ability to perform many tasks in a zero-shot manner [34, 26, 62,  
50 61, 70, 35, 18], strong control over the generation process [14, 47, 72, 38, 17, 48], natural robustness  
51 to noise in images [62, 26, 12, 63], and the ability to achieve image-to-image translation [73, 8, 18,  
52 37, 55, 12, 27, 35]. We were pleasantly surprised to find that these properties perfectly match the  
53 goals we mentioned above for image steganography: (1) **Security**: By utilizing the DDIM Inversion  
54 technique [52] for diffusion-based image translation, we ensure the invertibility of the translation  
55 process. This invertible translation process enables a coverless steganography framework, ensuring  
56 the security of the hidden image. (2) **Controllability**: The powerful control capabilities of conditional  
57 diffusion models make the container image highly controllable, and its visual quality is guaranteed  
58 by the generative prior of the diffusion model; (3) **Robustness**: Diffusion models are essentially  
59 Gaussian denoisers and have natural robustness to noise and perturbations. Even if the container  
60 image is degraded during transmission, we can still reveal the main content of the secret image.

61 We believe that the fusion of diffusion models and image steganography is not simply a matter of  
62 mechanically combining them, but rather an elegant and instructive integration that takes into account  
63 the real concerns of image steganography. Based on these ideas, we propose the **Controllable, Robust**  
64 and **Secure Image Steganography (CRoSS)** framework, a new image steganography framework that  
65 aims to simultaneously achieve gains in security, controllability, and robustness.

66 Our contributions can be summarized as follows:

- 67 • We identify the limitations of existing image steganography methods and propose a unified goal of  
68 achieving security, controllability, and robustness. We also demonstrate that the diffusion model  
69 can seamlessly integrate with image steganography to achieve these goals using diffusion-based  
70 invertible image translation technique without requiring any additional training.
- 71 • We propose a new image steganography framework: Controllable, Robust and Secure Image  
72 Steganography (CRoSS). To the best of our knowledge, this is the first attempt to apply the  
73 diffusion model to the field of image steganography and gain better performance.
- 74 • We leveraged the progress of the rapidly growing Stable Diffusion community to propose variants  
75 of CRoSS using prompts, LoRAs, and ControlNets, enhancing its controllability and diversity.
- 76 • We conducted comprehensive experiments focusing on the three targets of security, controllability,  
77 and robustness, demonstrating the advantages of CRoSS compared to existing methods.

## 78 2 Related Work

### 79 2.1 Steganography Methods

80 **Cover-based Image Steganography.** Unlike cryptography, steganography aims to hide secret  
81 data in a host to produce an information container. For image steganography, a cover image is  
82 required to hide the secret image in it [5]. Traditionally, spatial-based [22, 39, 41, 44] methods  
83 utilize the Least Significant Bits (LSB), pixel value differencing (PVD) [41], histogram shifting [58],  
84 multiple bit-planes [39] and palettes [22, 40] to hide images, which may arise statistical suspicion  
85 and are vulnerable to steganalysis methods. Adaptive methods [43, 29] decompose the steganography  
86 into embedding distortion minimization and data coding, which is indistinguishable by appearance  
87 but limited in capacity. Various transform-based schemes [10, 25] including JSteg [44] and DCT  
88 steganography [19] also fail to offer high payload capacity. Recently, various deep learning-based  
89 schemes have been proposed to solve image steganography. Baluja [5] proposed the first deep-  
90 learning method to hide a full-size image into another image. Generative adversarial networks  
91 (GANs) [51] are introduced to synthesize container images. Probability map methods focus on

92 generating various cost functions satisfying minimal-distortion embedding [43, 57]. [67] proposes  
 93 a generator based on U-Net. [56] presents an adversarial scheme under distortion minimization.  
 94 Three-player game methods like SteganoGAN [71] and HiDDeN [75] learn information embedding  
 95 and recovery by auto-encoder architecture to adversarially resist steganalysis. Recent attempts [64] to  
 96 introduce invertible neural networks (INN) into low-level inverse problems like denoising, rescaling,  
 97 and colorization show impressive potential over auto-encoder, GAN [3], and other learning-based  
 98 architectures. Recently, [33, 24] proposed designing the steganography model as an invertible neural  
 99 network (INN) [15, 16] to perform image hiding and recovering with a single INN model.

100 **Coverless Steganography.** Coverless steganography is an emerging technique in the field of  
 101 information hiding, which aims to embed secret information within a medium without modifying the  
 102 cover object [45]. Unlike traditional steganography methods that require a cover medium (e.g., an  
 103 image or audio file) to be altered for hiding information, coverless steganography seeks to achieve  
 104 secure communication without introducing any changes to the cover object [31]. This makes it more  
 105 challenging for adversaries to detect the presence of hidden data, as there are no observable changes  
 106 in the medium's properties [36]. To the best of our knowledge, existing coverless steganography  
 107 methods [32] still focus on hiding bits into container images, and few explorations involve hiding  
 108 images without resorting to cover images.

## 109 2.2 Diffusion Models

110 Diffusion models [20, 53, 54] are a type of generative model that is trained to learn the target image  
 111 distribution from a noise distribution. Recently, due to their powerful generative capabilities, diffusion  
 112 models have been widely used in various image applications, including image generation [14, 46,  
 113 49, 47], restoration [50, 26, 62], translation [12, 27, 35, 73], and more. Large-scale diffusion model  
 114 communities have also emerged on the Internet, with the aim of promoting the development of  
 115 AIGC(AI-generated content)-related fields by applying the latest advanced techniques.

116 In these communities, the Stable Diffusion [47] community is currently one of the most popular and  
 117 thriving ones, with a large number of open-source tools available for free, including model checkpoints  
 118 finetuned on various specialized datasets. Additionally, various LoRAs [21] and ControlNets [72] are  
 119 available in these communities for efficient control over the results generated by Stable Diffusion.  
 120 LoRAs achieve control by efficiently modifying some network parameters in a low-rank way, while  
 121 ControlNets introduce an additional network to modify the intermediate features of Stable Diffusion  
 122 for control. These mentioned recent developments have enhanced our CRoSS framework.

## 123 3 Method

### 124 3.1 Definition of Image Steganography

125 Before introducing our specific method, we first define the  
 126 image steganography task as consisting of three images  
 127 and two processes (as shown in Fig. 1): the three images  
 128 refer to the secret image  $\mathbf{x}_{sec}$ , container image  $\mathbf{x}_{cont}$ , and  
 129 revealed image  $\mathbf{x}_{rev}$ , while the two processes are the hide  
 130 process and reveal process. The secret image  $\mathbf{x}_{sec}$  is the  
 131 image we want to hide and is hidden in the container  
 132 image  $\mathbf{x}_{cont}$  through the hide process. After transmission  
 133 over the Internet, the container image  $\mathbf{x}_{cont}$  may become  
 134 degraded, resulting in a degraded container image  $\mathbf{x}'_{cont}$ ,  
 135 from which we extract the revealed image  $\mathbf{x}_{rev}$  through  
 136 the reveal process. Our goal is to make our proposed framework have the following properties: (1)  
 137 **Security:** even if the container image  $\mathbf{x}_{cont}$  is intercepted by other receivers, the hidden secret image  
 138  $\mathbf{x}_{sec}$  cannot be leaked. (2) **Controllability:** the content in the container image  $\mathbf{x}_{cont}$  can be controlled  
 139 by the user, and its visual quality is high. (3) **Robustness:** the reveal process can still generate  
 140 semantically consistent results ( $\mathbf{x}_{rev} \approx \mathbf{x}_{sec}$ ) even if there is deviation in the  $\mathbf{x}'_{cont}$  compared to the  
 141  $\mathbf{x}_{cont}$  ( $\mathbf{x}'_{cont} = d(\mathbf{x}_{cont})$ ,  $d(\cdot)$  denotes the degradation process). According to the above definition,  
 142 we can consider the hide process as a translation between the secret image  $\mathbf{x}_{sec}$  and the container  
 143 image  $\mathbf{x}_{cont}$ , and the reveal process as the inverse process of the hide process. In Sec. 3.2, we will

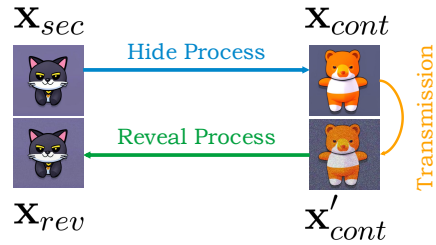


Figure 1: Illustration used to show the definition of image steganography.

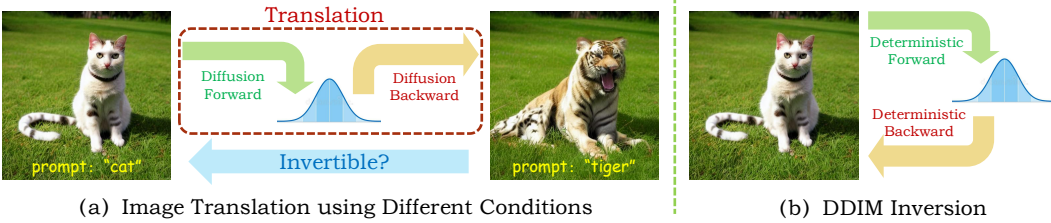


Figure 2: In part (a), Conditional diffusion models can be used with different conditions to perform image translation. In this example, we use two different prompts (“cat” and “tiger”) to translate a cat image into a tiger image. However, a critical challenge for coverless image steganography is whether we can reveal the original image from the translated image. The answer is yes, and we can use DDIM Inversion (shown in part (b)) to achieve dual-direction translation between the image distribution and noise distribution, allowing for invertible image translation.

144 introduce how to use diffusion models to implement these ideas, and in Sec. 3.3, we will provide a  
 145 detailed description of our proposed framework CRoSS for coverless image steganography.

### 146 3.2 Invertible Image Translation using Diffusion Model

147 **Diffusion Model Defined by DDIM.** A complete diffusion model process consists of two stages:  
 148 the forward phase adds noise to a clean image, while the backward sampling phase denoises it step  
 149 by step. In DDIM [52], the formula for the forward process is given by:

$$\mathbf{x}_t = \sqrt{\alpha_t} \mathbf{x}_{t-1} + \sqrt{1 - \alpha_t} \boldsymbol{\epsilon}, \quad \boldsymbol{\epsilon} \sim \mathcal{N}(\mathbf{0}, \mathbf{I}), \quad (1)$$

150 where  $\mathbf{x}_t$  denotes the noisy image in the  $t$ -th step,  $\boldsymbol{\epsilon}$  denotes the randomly sampled Gaussian noise,  
 151  $\alpha_t$  is a predefined parameter and the range of time step  $t$  is  $[1, T]$ . The formula of DDIM for the  
 152 backward sampling process is given by:

$$\mathbf{x}_s = \sqrt{\bar{\alpha}_s} \mathbf{f}_{\boldsymbol{\theta}}(\mathbf{x}_t, t) + \sqrt{1 - \bar{\alpha}_s - \sigma_s^2} \boldsymbol{\epsilon}_{\boldsymbol{\theta}}(\mathbf{x}_t, t) + \sigma_s \boldsymbol{\epsilon}, \quad \mathbf{f}_{\boldsymbol{\theta}}(\mathbf{x}_t, t) = \frac{\mathbf{x}_t - \sqrt{1 - \bar{\alpha}_t} \boldsymbol{\epsilon}_{\boldsymbol{\theta}}(\mathbf{x}_t, t)}{\sqrt{\bar{\alpha}_t}}, \quad (2)$$

153 where  $\boldsymbol{\epsilon} \sim \mathcal{N}(\mathbf{0}, \mathbf{I})$  is a randomly sampled Gaussian noise with  $\sigma_s^2$  as the noise variance,  $\mathbf{f}_{\boldsymbol{\theta}}(\cdot, t)$  is a  
 154 denoising function based on the pre-trained noise estimator  $\boldsymbol{\epsilon}_{\boldsymbol{\theta}}(\cdot, t)$ , and  $\bar{\alpha}_t = \prod_{i=1}^t \alpha_i$ . DDIM does  
 155 not require the two steps in its sampling formula to be adjacent (i.e.,  $t = s + 1$ ). Therefore,  $s$  and  
 156  $t$  can be any two steps that satisfy  $s < t$ . This makes DDIM a popular algorithm for accelerating  
 157 sampling. Furthermore, if  $\sigma_s$  in Eq.2 is set to 0, the DDIM sampling process becomes deterministic.  
 158 In this case, the sampling result is solely determined by the initial value  $\mathbf{x}_T$ , which can be considered  
 159 as a latent code. The sampling process can also be equivalently described as solving an Ordinary  
 160 Differential Equation (ODE) using an ODE solver [52]. In our work, we choose deterministic DDIM  
 161 to implement the diffusion model and use the following formula:

$$\mathbf{x}_0 = \text{ODESolve}(\mathbf{x}_T; \boldsymbol{\epsilon}_{\boldsymbol{\theta}}, T, 0) \quad (3)$$

162 to represent the process of sampling from  $\mathbf{x}_T$  to  $\mathbf{x}_0$  using a pretrained noise estimator  $\boldsymbol{\epsilon}_{\boldsymbol{\theta}}$ .

163 **Image Translation using Diffusion Model.** A large number of image translation methods [73, 8,  
 164 18, 37, 55, 12, 27, 35] based on diffusion models have been proposed. In our method, we will adopt  
 165 a simple approach. First, we assume that the diffusion models used in our work are all conditional  
 166 diffusion models that support condition  $c$  as input to control the generated results. Taking the example  
 167 shown in Fig. 2 (a), suppose we want to transform an image of a cat into an image of a tiger. We add  
 168 noise to the cat image using the forward process (Eq. 1) to obtain the intermediate noise, and then  
 169 control the backward sampling process (Eq. 2) from noise by inputting a condition (prompt=“tiger”),  
 170 resulting in a new tiger image. In general, if the sampling condition is set to  $c$ , our conditional  
 171 sampling process can be expressed based on Eq. 3 as follows:

$$\mathbf{x}_0 = \text{ODESolve}(\mathbf{x}_T; \boldsymbol{\epsilon}_{\boldsymbol{\theta}}, c, T, 0). \quad (4)$$

172 For image translation, there are two properties that need to be considered: the structural consistency  
 173 of the two images before and after the translation, and whether the translation process is invertible.  
 174 Structural consistency is crucial for most applications related to image translation, but for coverless  
 175 image steganography, ensuring the invertibility of the translation process is the more important goal.  
 176 To achieve invertible image translation, we utilize DDIM Inversion based on deterministic DDIM.

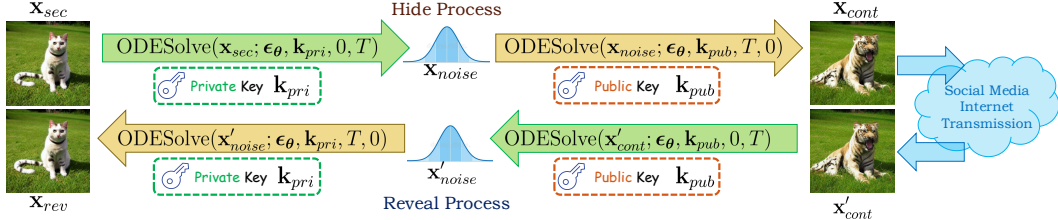


Figure 3: Our coverless image steganography framework CRoSS. The diffusion model we choose is a conditional diffusion model, which supports conditional inputs to control the generation results. We choose the deterministic DDIM as the sampling strategy and use the two different conditions ( $k_{pri}$  and  $k_{pub}$ ) given to the model as the private key and the public key.

---

**Algorithm 1** The Hide Process of CRoSS.

---

**Input:** The secret image  $x_{sec}$  which will be hided, a pre-trained conditional diffusion model with noise estimator  $\epsilon_\theta$ , the number  $T$  of time steps for sampling and two different conditions  $k_{pri}$  and  $k_{pub}$  which serve as the private and public keys.  
**Output:** The container image  $x_{cont}$  used to hide the secret image  $x_{sec}$ .  
 $x_{noise} = \text{ODESolve}(x_{sec}; \epsilon_\theta, k_{pri}, 0, T)$   
 $x_{cont} = \text{ODESolve}(x_{noise}; \epsilon_\theta, k_{pub}, T, 0)$   
**return**  $x_{cont}$

---

177 **DDIM Inversion Makes an Invertible Image Translation.** DDIM Inversion (shown in Fig. 2  
178 (b)), as the name implies, refers to the process of using DDIM to achieve the conversion from an  
179 image to a latent noise and back to the original image. The idea is based on the approximation of  
180 forward and backward differentials in solving ordinary differential equations [52, 27]. Intuitively, in  
181 the case of deterministic DDIM, it allows  $s$  and  $t$  in Eq. 2 to be any two steps (i.e., allowing  $s < t$   
182 and  $s > t$ ). When  $s < t$ , Eq. 2 performs the backward process, and when  $s > t$ , Eq. 2 performs the  
183 forward process. As the trajectories of forward and backward processes are similar, the input and  
184 output images are very close, and the intermediate noise  $x_T$  can be considered as the latent variable  
185 of the inversion. In our work, we use the following formulas:

$$x_T = \text{ODESolve}(x_0; \epsilon_\theta, c, 0, T), \quad x'_0 = \text{ODESolve}(x_T; \epsilon_\theta, c, T, 0), \quad (5)$$

186 to represent the DDIM Inversion process from the original image  $x_0$  to the latent code  $x_T$  and from  
187 the latent code  $x_T$  back to the original image  $x_0$  (the output image is denoted as  $x'_0$  and  $x'_0 \approx x_0$ ).  
188 Based on DDIM Inversion, we have achieved the invertible relationship between images and latent  
189 noises. As long as we use deterministic DDIM to construct the image translation framework, the  
190 entire framework can achieve invertibility with two DDIM Inversion loops. It is the basis of our  
191 coverless image steganography framework, which will be described in detail in the next subsection.

192 **3.3 The Coverless Image Steganography Framework CRoSS**

193 Our basic framework CRoSS is based on a conditional diffusion model, whose noise estimator is  
194 represented by  $\epsilon_\theta$ , and two different conditions that serve as inputs to the diffusion model. In our  
195 work, these two conditions can serve as the private key and public key (denoted as  $k_{pri}$  and  $k_{pub}$ ), as  
196 shown in Fig.3, with detailed workflow described in Algo.1 and Algo. 2. We will introduce the entire  
197 CRoSS framework in two parts: the hide process and the reveal process.

198 **The Process of Hide Stage.** In the hide stage, we attempt to perform translation between the  
199 secret image  $x_{sec}$  and the container image  $x_{cont}$  using the forward and backward processes of  
200 deterministic DDIM. In order to make the images before and after the translation different, we use  
201 the pre-trained conditional diffusion model with different conditions in the forward and backward  
202 processes respectively. These two different conditions also serve as private and public keys in the  
203 CRoSS framework. Specifically, the private key  $k_{pri}$  is used for the forward process, while the  
204 public key  $k_{pub}$  is used for the backward process. After getting the container image  $x_{cont}$ , it will be  
205 transmitted over the Internet and publicly accessible to all potential receivers.

---

**Algorithm 2** The Reveal Process of CRoSS.

---

**Input:** The container image  $\mathbf{x}'_{cont}$  that has been transmitted over the Internet (may be degraded from  $\mathbf{x}_{cont}$ ), the pre-trained conditional diffusion model with noise estimator  $\epsilon_\theta$ , the number  $T$  of time steps for sampling, the private key  $\mathbf{k}_{pri}$  and public key  $\mathbf{k}_{pub}$ .

**Output:** The revealed image  $\mathbf{x}_{rev}$ .

$$\mathbf{x}'_{noise} = \text{ODESolve}(\mathbf{x}'_{cont}; \epsilon_\theta, \mathbf{k}_{pub}, 0, T)$$

$$\mathbf{x}_{rev} = \text{ODESolve}(\mathbf{x}'_{noise}; \epsilon_\theta, \mathbf{k}_{pri}, T, 0)$$

**return**  $\mathbf{x}_{rev}$

---

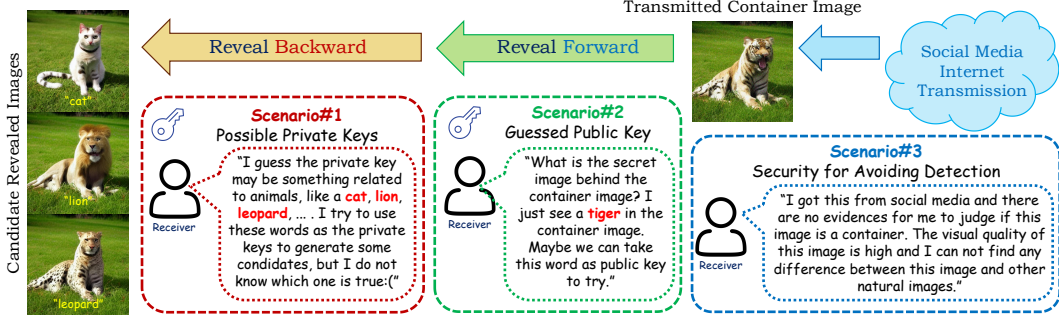


Figure 4: Further explanation of the CRoSS framework. We simulated the possible problems that a receiver may encounter in three different scenarios during the reveal process.

206    **The Roles of the Private and Public Keys in Our CRoSS Framework.** In CRoSS, we found  
 207    that these given conditions can act as keys in practical use. The private key is used to describe  
 208    the content in the secret image, while the public key is used to control the content in the container  
 209    image. For the public key, it is associated with the content in the container image, so even if it is  
 210    not manually transmitted over the network, the receiver can guess it based on the received container  
 211    image (described in Scenario#2 of Fig. 4). For the private key, it determines whether the receiver can  
 212    successfully reveal the original image, so it cannot be transmitted over public channels.

213    **The Process of Reveal Stage.** In the reveal stage, assuming that the container image has been  
 214    transmitted over the Internet and may have been damaged as  $\mathbf{x}'_{cont}$ , the receiver needs to reveal it  
 215    back to the secret image through the same forward and backward process using the same conditional  
 216    diffusion model with corresponding keys. Throughout the entire coverless image steganography  
 217    process, we do not train or fine-tune the diffusion models specifically for image steganography tasks,  
 218    but rely on the inherent invertible image translation guaranteed by the DDIM Inversion.

219    **The Security Guaranteed by CRoSS.** Some questions about security may be raised, such as:  
 220    What if the private key is guessed by the receivers? Does the container image imply the possible  
 221    hidden secret image? We clarify these questions from two aspects: (1) Since the revealed image is  
 222    generated by the diffusion model, the visual quality of the revealed image is relatively high regardless  
 223    of whether the input private key is correct or not. The receiver may guess the private key by exhaustive  
 224    method, but it is impossible to judge which revealed image is the true secret image from a pile of  
 225    candidate revealed images (described in Scenario#1 of Fig. 4). (2) Since the container image is  
 226    also generated by the diffusion model, its visual quality is guaranteed by the generative prior of the  
 227    diffusion model. Moreover, unlike cover-based methods that explicitly store clues in the container  
 228    image, the container image in CRoSS does not contain any clues that can be detected or used to extract  
 229    the secret image. Therefore, it is hard for the receiver to discover that the container image hides other  
 230    images or to reveal the secret image using some detection method (described in Scenario#3 of Fig. 4).

231    **Various Variants for Public and Private Keys.** Our proposed CRoSS relies on pre-trained con-  
 232    ditional diffusion models with different conditions  $\mathbf{k}_{pub}$ ,  $\mathbf{k}_{pri}$  and these conditions serve as keys in  
 233    the CRoSS framework. In practical applications, we can distinguish different types of conditions of  
 234    diffusion models in various ways. Here are some examples: (1) **Prompts**: using the same checkpoint  
 235    of text-to-image diffusion models like Stable Diffusion [47] but different prompts as input condi-  
 236    tions; (2) **LoRAs** [21]: using the same checkpoint initialization, but loading different LoRAs; (3)  
 237    **ControlNets** [72]: loading the same checkpoint but using ControlNet with different conditions.

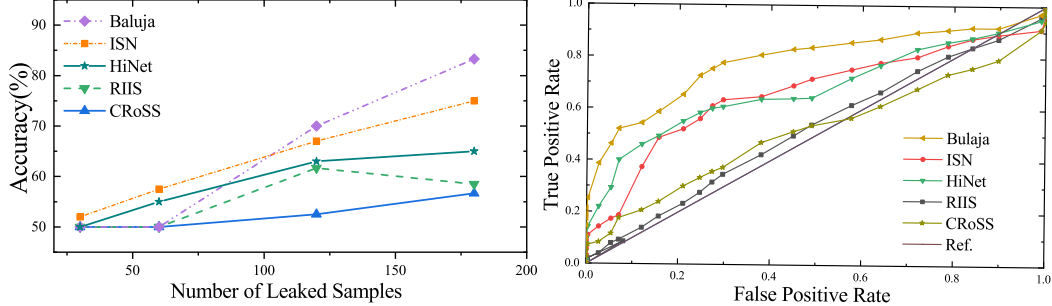


Figure 5: Deep steganalysis results by the latest SID [59]. As the number of leaked samples increases, methods whose detection accuracy curves grow more slowly and approach 50% exhibit higher security. The right is the recall curve of different methods under the StegExpose [7] detector. The closer the area enclosed by the curve and the coordinate axis is to 0.5, the closer the method is to the ideal evasion of the detector.

## 238 4 Experiment

### 239 4.1 Implementation Details

240 **Experimental Settings.** In our experiment, we chose Stable Diffusion [47] v1.5 as the conditional  
 241 diffusion model, and we used the deterministic DDIM [52] sampling algorithm. Both the forward  
 242 and backward processes consisted of 50 steps. To achieve invertible image translation, we set the  
 243 guidance scale of Stable Diffusion to 1. For the given conditions, which serve as the private and  
 244 public keys, we had three options: prompts, conditions for ControlNets [72] (depth maps, scribbles,  
 245 segmentation maps), and LoRAs [21]. All experiments were conducted on a GeForce RTX 3090  
 246 GPU card, and our method did not require any additional training or fine-tuning for the diffusion  
 247 model. The methods we compared include RIIS [66], HiNet [24], Baluja [6], and ISN [33].

248 **Data Preparation.** To perform a quantitative and qualitative analysis of our method, we collect a  
 249 benchmark with a total of 260 images and generate corresponding prompt keys specifically tailored  
 250 for the coverless image steganography, dubbed Stego260. We categorize the dataset into three classes,  
 251 namely humans, animals, and general objects (such as architecture, plants, food, furniture, etc.). The  
 252 images in the dataset are sourced from publicly available datasets [1, 2] and Google search engines.  
 253 For generating prompt keys, we utilize BLIP [30] to generate private keys and employ ChatGPT or  
 254 artificial adjustment to perform semantic modifications and produce public keys in batches. More  
 255 details about the dataset can be found in the supplementary material.

### 256 4.2 Property Study#1: Security

257 In Fig. 5, the recent learning-based steganalysis  
 258 method Size-Independent-Detector (SID) [59]  
 259 is retrained with leaked samples from testing  
 260 results of various methods on Stego260. The  
 261 detection accuracy of CRoSS increases more  
 262 gradually as the number of leaked samples rises,  
 263 compared to other methods. The recall curves  
 264 on the right also reveal the lower detection ac-  
 265 curacy of our CRoSS, indicating superior anti-  
 266 steganalysis performance.

267 Our security encompasses two aspects: imper-  
 268 ceptibility in visual quality against human suspi-  
 269 cion and resilience against steganalysis attacks.

270 NIQE is a no-reference image quality assessment (IQA)  
 271 model to measure the naturalness and visual  
 272 security without any reference image or human feedback. In Tab. 1, the lower the NIQE score, the  
 273 less likely it is for the human eye to identify the image as a potentially generated container for hiding  
 274 secret information. Our NIQE is close to those of other methods, as well as the original input image  
 275 (2.85), making it difficult to discern with human suspicion. Anti-analysis security is evaluated by  
 three steganalysis models XuNet[65], YedroudjNet[68], and KeNet[69], for which lower detection

Methods	NIQE ↓	Detection Accuracy - 50  ↓		
		XuNet [65]	YedroudjNet [68]	KeNet [69]
Baluja [6]	3.43±0.08	45.18±1.69	43.12±2.18	46.88±2.37
ISN [33]	<b>2.87±0.02</b>	5.14±0.44	3.01±0.29	8.62±1.19
HiNet [24]	<b>2.94±0.02</b>	5.29±0.44	3.12±0.36	8.33±1.22
RIIS [66]	3.13±0.05	<b>0.73±0.13</b>	<b>0.24±0.08</b>	<b>4.88±1.15</b>
CRoSS (ours)	3.04	<b>1.32</b>	<b>0.18</b>	<b>2.11</b>

Table 1: Security analysis. NIQE indicates the visual quality of container images, lower is better. The closer the detection rate of a method approximates 50%, the more secure the method is considered, as it suggests its output is indistinguishable from random chance. The best results are red and the second-best results are blue.

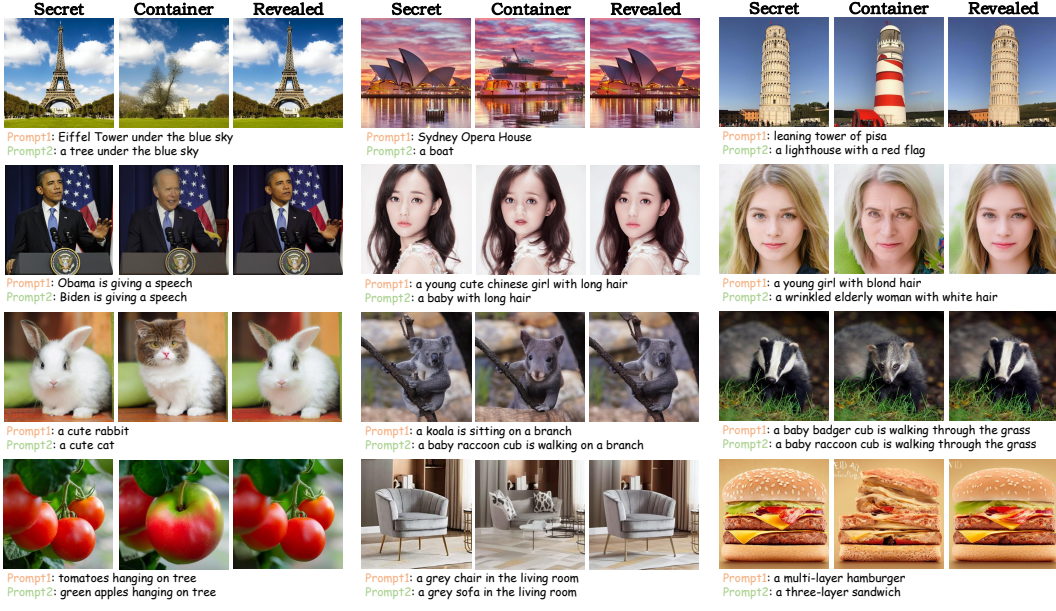


Figure 6: Visual results of the proposed CRoSS controlled by different prompts. The container images are realistic and the revealed images have well semantic consistency with the secret images.

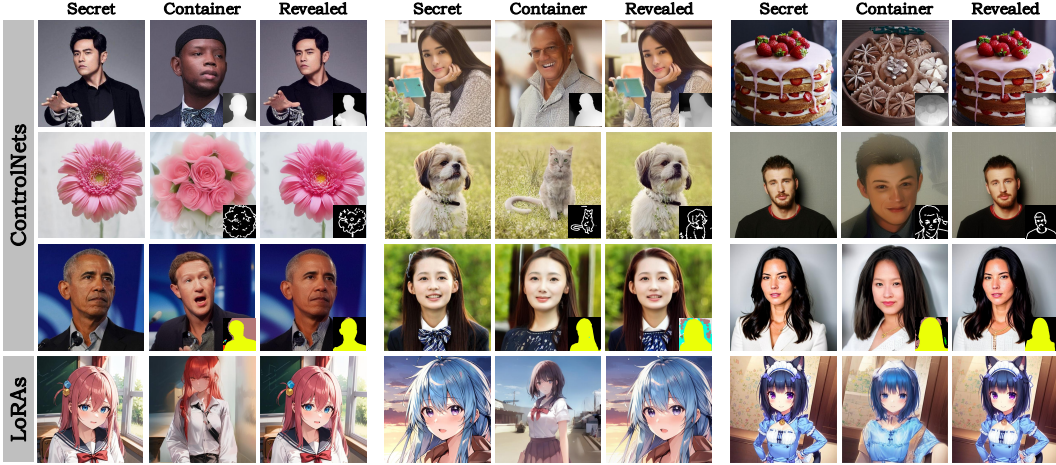


Figure 7: Visual results of our CRoSS controlled by different ControlNets and LoRAs. Depth maps, scribbles, and segmentation maps are presented in the lower right corner of the images.

accuracy denotes higher security. Our CRoSS demonstrates the highest or near-highest resistance against various steganalysis methods.

### 4.3 Property Study#2: Controllability

To verify the controllability and flexibility of the proposed CRoSS, various types of private and public keys such as prompts, ControlNets, and LoRAs<sup>2</sup> are incorporated in our framework. As illustrated in Fig. 6, our framework is capable of effectively hiding the secret images in the container images based on the user-provided “Prompt2” without noticeable artifacts or unrealistic image details. The container image allows for the seamless modification of a person’s identity information, facial attributes, as well as species of animals. The concepts of these two prompts can also differ significantly such as the Eiffel Tower and a tree, thereby enhancing the concealment capability and stealthiness of the container images. Meanwhile, the revealed image extracted with “Prompt1” exhibits well fidelity by accurately preserving the semantic information of secret images. Besides prompts, our CRoSS also supports the utilization of various other control conditions as keys, such as depth maps, scribbles, and

<sup>2</sup>The last row of Fig. 7 are generated via LoRAs downloaded from <https://civitai.com/>.

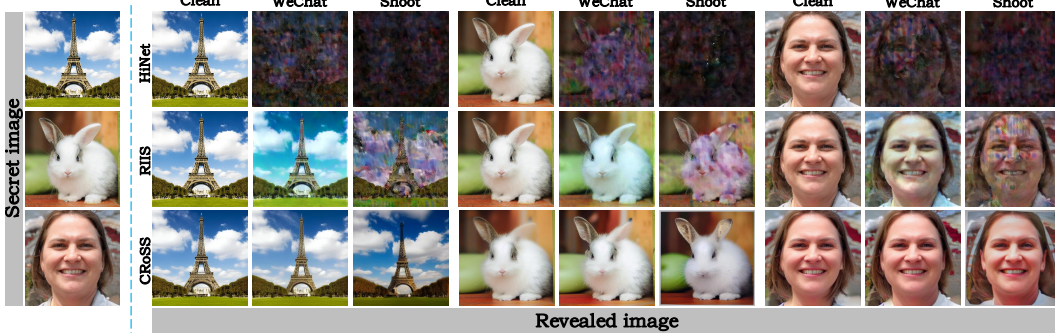


Figure 8: Visual comparisons of our CRoSS and other methods [66, 24] under two real-world degradations, namely “WeChat” and “Shoot”. Obviously, our method can reconstruct the content of secret images, while other methods exhibit significant color distortion or have completely failed.

Methods	clean	Gaussian noise			Gaussian denoiser [60]			JPEG compression			JPEG enhancer [60]		
		$\sigma = 10$	$\sigma = 20$	$\sigma = 30$	$\sigma = 10$	$\sigma = 20$	$\sigma = 30$	$Q = 20$	$Q = 40$	$Q = 80$	$Q = 20$	$Q = 40$	$Q = 80$
Baluja [6]	34.24	10.30	7.54	6.92	7.97	6.10	5.49	6.59	8.33	11.92	5.21	6.98	9.88
ISN [33]	41.83	12.75	10.98	9.93	11.94	9.44	6.65	7.15	9.69	13.44	5.88	8.08	11.63
HiNet [24]	42.98	12.91	11.54	10.23	11.87	9.32	6.87	7.03	9.78	13.23	5.59	8.21	11.88
RIIS [66]	43.78	26.03	18.89	15.85	20.89	15.97	13.92	22.03	25.41	27.02	13.88	16.74	20.13
CRoSS (ours)	23.79	21.89	20.19	18.77	21.39	21.24	21.02	21.74	22.74	23.51	20.60	21.22	21.19

Table 2: PSNR(dB) results of the proposed CRoSS and other methods under different levels of degradations. The proposed CRoSS can achieve superior data fidelity in most settings. The best results are red and the second-best results are blue.

289 segmentation maps. As depicted in Fig. 7, our methods can effectively hide and reveal the semantic  
290 information of the secret image without significantly compromising the overall visual quality or  
291 arousing suspicion. Our CRoSS can also adopt different LoRAs as keys, which is conducive to  
292 personalized image steganography.

#### 293 4.4 Property Study#3: Robustness

294 **Simulation Degradation.** To validate the robustness of our method, we conduct experiments on  
295 simulation degradation such as Gaussian noise and JPEG compression. As reported in Tab. 2, our  
296 CRoSS performs excellent adaptability to various levels of degradation with minimal performance  
297 decrease, while other methods suffer significant drops in fidelity (over 20dB in PSNR). Meanwhile,  
298 our method achieves the best PSNR at  $\sigma = 20$  and  $\sigma = 30$ . Furthermore, when we perform nonlinear  
299 image enhancement [60] on the degraded container images, all other methods have deteriorations but  
300 our CRoSS can still maintain good performance and achieve improvements in the Gaussian noise  
301 degradation. Noting that RIIS [66] is trained exclusively on degraded data, but our CRoSS is naturally  
302 resistant to various degradations in a zero-shot manner and outperforms RIIS in most scenarios.

303 **Real-World Degradation.** We further choose two real-world degradations including “WeChat” and  
304 “Shoot”. Specifically, we send and receive container images via the pipeline of WeChat to implement  
305 network transmission. Simultaneously, we utilize the mobile phone to capture the container images  
306 on the screen and then simply crop and warp them. Obviously, as shown in Fig. 8, all other methods  
307 have completely failed or present severe color distortion subjected to these two extremely complex  
308 degradations, yet our method can still reveal the approximate content of the secret images and  
309 maintain well semantic consistency, which proves the superiority of our method.

## 310 5 Conclusion

311 We propose a coverless image steganography framework named CRoSS (Controllable, Robust, and  
312 Secure Image Steganography) based on diffusion models. This framework leverages the unique  
313 properties of diffusion models and demonstrates superior performance in terms of security, control-  
314 lability, and robustness compared to existing methods. To the best of our knowledge, CRoSS is  
315 the first attempt to integrate diffusion models into the field of image steganography. In the future,  
316 diffusion-based image steganography techniques will continue to evolve, expanding their capacity  
317 and improving fidelity while maintaining their existing advantages.

318 **References**

- 319 [1] [https://github.com/aisegmentcn/matting\\_human\\_datasets](https://github.com/aisegmentcn/matting_human_datasets), 2019.
- 320 [2] <https://www.kaggle.com/datasets/iamsouravbanerjee/animal-image-dataset-90-different-animals>, 2022.
- 321 [3] Rameen Abdal, Yipeng Qin, and Peter Wonka. Image2stylegan: How to embed images into the stylegan latent space? In *Proceedings of the IEEE/CVF International Conference on Computer Vision (ICCV)*, pages 4432–4441, 2019.
- 322 [4] Alaa A Jabbar Altaay, Shahrin Bin Sahib, and Mazdak Zamani. An introduction to image steganography techniques. In *2012 International Conference on Advanced Computer Science Applications and Technologies (ACSAT)*, pages 122–126. IEEE, 2012.
- 323 [5] Shumeet Baluja. Hiding images in plain sight: Deep steganography. In *NeurIPS*, 2017.
- 324 [6] Shumeet Baluja. Hiding images within images. *TPAMI*, 2019.
- 325 [7] Benedikt Boehm. StegExpose-a tool for detecting lsb steganography. *arXiv preprint arXiv:1410.6656*, 2014.
- 326 [8] Tim Brooks, Aleksander Holynski, and Alexei A Efros. Instructpix2pix: Learning to follow image editing instructions. *arXiv preprint arXiv:2211.09800*, 2022.
- 327 [9] Chi-Kwong Chan and Lee-Ming Cheng. Hiding data in images by simple lsb substitution. *PR*, 2004.
- 328 [10] Yambem Jina Chanu, Kh Manglem Singh, and Themrichon Tuithung. Image steganography and steganalysis: A survey. In *IJCAI*, 2012.
- 329 [11] Abbas Cheddad, Joan Condell, Kevin Curran, and Paul Mc Kevitt. Digital image steganography: Survey and analysis of current methods. *IEEE Transactions on Signal Processing*, 2010.
- 330 [12] Jooyoung Choi, Sungwon Kim, Yonghyun Jeong, Youngjune Gwon, and Sungroh Yoon. Ilvr: Conditioning method for denoising diffusion probabilistic models. In *Proceedings of the IEEE/CVF International Conference on Computer Vision (ICCV)*, 2021.
- 331 [13] Ingemar Cox, Matthew Miller, Jeffrey Bloom, Jessica Fridrich, and Ton Kalker. *Digital watermarking and steganography*. Morgan kaufmann, 2007.
- 332 [14] Prafulla Dhariwal and Alexander Nichol. Diffusion models beat gans on image synthesis. In *Advances in Neural Information Processing Systems (NeurIPS)*, 2021.
- 333 [15] Laurent Dinh, David Krueger, and Yoshua Bengio. Nice: Non-linear independent components estimation. *arXiv preprint arXiv:1410.8516*, 2014.
- 334 [16] Laurent Dinh, Jascha Sohl-Dickstein, and Samy Bengio. Density estimation using real NVP. In *Proceedings of the International Conference on Learning Representations (ICLR)*, 2017.
- 335 [17] Rinon Gal, Yuval Alaluf, Yuval Atzmon, Or Patashnik, Amit H. Bermano, Gal Chechik, and Daniel Cohen-Or. An image is worth one word: Personalizing text-to-image generation using textual inversion, 2022.
- 336 [18] Amir Hertz, Ron Mokady, Jay Tenenbaum, Kfir Aberman, Yael Pritch, and Daniel Cohen-Or. Prompt-to-prompt image editing with cross attention control. *arXiv preprint arXiv:2208.01626*, 2022.
- 337 [19] Stefan Hetzl and Petra Mutzel. A graph-theoretic approach to steganography. In *IFIP International Conference on Communications and Multimedia Security*, 2005.
- 338 [20] Jonathan Ho, Ajay Jain, and Pieter Abbeel. Denoising diffusion probabilistic models. In *Advances in Neural Information Processing Systems (NeurIPS)*, 2020.

- 361 [21] Edward J Hu, yelong shen, Phillip Wallis, Zeyuan Allen-Zhu, Yuanzhi Li, Shean Wang,  
 362 Lu Wang, and Weizhu Chen. LoRA: Low-rank adaptation of large language models. In  
 363 *International Conference on Learning Representations*, 2022.
- 364 [22] Shoko Imaizumi and Kei Ozawa. Multibit embedding algorithm for steganography of palette-  
 365 based images. In *PSIVT*, 2013.
- 366 [23] Priyank Jaini, Kira A Selby, and Yaoliang Yu. Sum-of-squares polynomial flow. In *ICML*, 2019.
- 367 [24] Junpeng Jing, Xin Deng, Mai Xu, Jianyi Wang, and Zhenyu Guan. Hinet: Deep image hiding  
 368 by invertible network. In *ICCV*, 2021.
- 369 [25] Inas Jawad Kadhim, Prashan Premaratne, Peter James Vial, and Brendan Halloran. Compre-  
 370 hensive survey of image steganography: Techniques, evaluations, and trends in future research.  
 371 *Neurocomputing*, 2019.
- 372 [26] Bahjat Kawar, Michael Elad, Stefano Ermon, and Jiaming Song. Denoising diffusion restoration  
 373 models. In *Advances in Neural Information Processing Systems (NeurIPS)*, 2022.
- 374 [27] Gwanghyun Kim, Taesung Kwon, and Jong Chul Ye. Diffusionclip: Text-guided diffusion  
 375 models for robust image manipulation. In *Proceedings of the IEEE/CVF Conference on*  
 376 *Computer Vision and Pattern Recognition (CVPR)*, 2022.
- 377 [28] Durk P Kingma, Tim Salimans, Rafal Jozefowicz, Xi Chen, Ilya Sutskever, and Max Welling.  
 378 Improved variational inference with inverse autoregressive flow. In *NeurIPS*, 2016.
- 379 [29] Bin Li, Ming Wang, Jiwu Huang, and Xiaolong Li. A new cost function for spatial image  
 380 steganography. In *ICIP*, 2014.
- 381 [30] Junnan Li, Dongxu Li, Caiming Xiong, and Steven Hoi. Blip: Bootstrapping language-  
 382 image pre-training for unified vision-language understanding and generation. In *International*  
 383 *Conference on Machine Learning*, pages 12888–12900. PMLR, 2022.
- 384 [31] Yung-Hui Li, Ching-Chun Chang, Guo-Dong Su, Kai-Lin Yang, Muhammad Saqlain Aslam,  
 385 and Yanjun Liu. Coverless image steganography using morphed face recognition based on  
 386 convolutional neural network. *EURASIP Journal on Wireless Communications and Networking*,  
 387 2022(1):1–21, 2022.
- 388 [32] Qiang Liu, Xuyu Xiang, Jiaohua Qin, Yun Tan, and Yao Qiu. Coverless image steganography  
 389 based on densenet feature mapping. *EURASIP Journal on Image and Video Processing*, 2020:1–  
 390 18, 2020.
- 391 [33] Shao-Ping Lu, Rong Wang, Tao Zhong, and Paul L Rosin. Large-capacity image steganography  
 392 based on invertible neural networks. In *CVPR*, 2021.
- 393 [34] Andreas Lugmayr, Martin Danelljan, Andres Romero, Fisher Yu, Radu Timofte, and Luc  
 394 Van Gool. Repaint: Inpainting using denoising diffusion probabilistic models. In *Proceedings*  
 395 *of the IEEE/CVF Conference on Computer Vision and Pattern Recognition (CVPR)*, 2022.
- 396 [35] Chenlin Meng, Yutong He, Yang Song, Jiaming Song, Jiajun Wu, Jun-Yan Zhu, and Stefano  
 397 Ermon. SDEdit: Guided image synthesis and editing with stochastic differential equations. In  
 398 *International Conference on Learning Representations*, 2022.
- 399 [36] Mohammed Saad Mohamed, EH Hafez, et al. Coverless image steganography based on jigsaw  
 400 puzzle image generation. *Computers, Materials and Continua*, 67(2):2077–2091, 2021.
- 401 [37] Ron Mokady, Amir Hertz, Kfir Aberman, Yael Pritch, and Daniel Cohen-Or. Null-text inversion  
 402 for editing real images using guided diffusion models. *arXiv preprint arXiv:2211.09794*, 2022.
- 403 [38] Chong Mou, Xintao Wang, Liangbin Xie, Jian Zhang, Zhongang Qi, Ying Shan, and Xiaohu Qie.  
 404 T2i-adapter: Learning adapters to dig out more controllable ability for text-to-image diffusion  
 405 models. *arXiv preprint arXiv:2302.08453*, 2023.
- 406 [39] Bui Cong Nguyen, Sang Moon Yoon, and Heung-Kyu Lee. Multi bit plane image steganography.  
 407 In *International Workshop on Digital Watermarking*, 2006.

- 408 [40] Michiharu Niimi, Hideki Noda, Eiji Kawaguchi, and Richard O Eason. High capacity and  
 409 secure digital steganography to palette-based images. In *ICIP*, 2002.
- 410 [41] Feng Pan, Jun Li, and Xiaoyuan Yang. Image steganography method based on pvd and modulus  
 411 function. In *ICECC*, 2011.
- 412 [42] George Papamakarios, Theo Pavlakou, and Iain Murray. Masked autoregressive flow for density  
 413 estimation. In *NeurIPS*, 2017.
- 414 [43] Tomáš Pevný, Tomáš Filler, and Patrick Bas. Using high-dimensional image models to perform  
 415 highly undetectable steganography. In *IHIP*, 2010.
- 416 [44] Niels Provos and Peter Honeyman. Hide and seek: An introduction to steganography. *IEEE*  
 417 *Symposium on Security and Privacy*, 2003.
- 418 [45] Jiaohua Qin, Yuanjing Luo, Xuyu Xiang, Yun Tan, and Huajun Huang. Coverless image  
 419 steganography: a survey. *IEEE Access*, 7:171372–171394, 2019.
- 420 [46] Aditya Ramesh, Prafulla Dhariwal, Alex Nichol, Casey Chu, and Mark Chen. Hierarchical  
 421 text-conditional image generation with clip latents. *arXiv preprint arXiv:2204.06125*, 2022.
- 422 [47] Robin Rombach, Andreas Blattmann, Dominik Lorenz, Patrick Esser, and Björn Ommer.  
 423 High-resolution image synthesis with latent diffusion models, 2021.
- 424 [48] Nataniel Ruiz, Yuanzhen Li, Varun Jampani, Yael Pritch, Michael Rubinstein, and Kfir Aberman.  
 425 Dreambooth: Fine tuning text-to-image diffusion models for subject-driven generation, 2023.
- 426 [49] Chitwan Saharia, William Chan, Saurabh Saxena, Lala Li, Jay Whang, Emily Denton, Seyed  
 427 Kamyar Seyed Ghaseimpour, Raphael Gontijo-Lopes, Burcu Karagol Ayan, Tim Salimans,  
 428 Jonathan Ho, David J. Fleet, and Mohammad Norouzi. Photorealistic text-to-image diffusion  
 429 models with deep language understanding. In Alice H. Oh, Alekh Agarwal, Danielle Belgrave,  
 430 and Kyunghyun Cho, editors, *Advances in Neural Information Processing Systems*, 2022.
- 431 [50] Chitwan Saharia, Jonathan Ho, William Chan, Tim Salimans, David J Fleet, and Mohammad  
 432 Norouzi. Image super-resolution via iterative refinement. *IEEE Transactions on Pattern Analysis  
 433 and Machine Intelligence*, 2022.
- 434 [51] Haichao Shi, Jing Dong, Wei Wang, Yinlong Qian, and Xiaoyu Zhang. Ssgan: secure steganog-  
 435 raphy based on generative adversarial networks. In *Pacific Rim Conference on Multimedia*,  
 436 2017.
- 437 [52] Jiaming Song, Chenlin Meng, and Stefano Ermon. Denoising diffusion implicit models. In  
 438 *International Conference on Learning Representations (ICLR)*, 2021.
- 439 [53] Yang Song and Stefano Ermon. Generative modeling by estimating gradients of the data  
 440 distribution. In *Advances in Neural Information Processing Systems (NeurIPS)*, 2019.
- 441 [54] Yang Song, Jascha Sohl-Dickstein, Diederik P Kingma, Abhishek Kumar, Stefano Ermon, and  
 442 Ben Poole. Score-based generative modeling through stochastic differential equations. In  
 443 *International Conference on Learning Representations (ICLR)*, 2021.
- 444 [55] Xuan Su, Jiaming Song, Chenlin Meng, and Stefano Ermon. Dual diffusion implicit bridges for  
 445 image-to-image translation. In *The Eleventh International Conference on Learning Representa-  
 446 tions*, 2023.
- 447 [56] Weixuan Tang, Bin Li, Shunquan Tan, Mauro Barni, and Jiwu Huang. Cnn-based adversarial  
 448 embedding for image steganography. *TIFS*, 2019.
- 449 [57] Weixuan Tang, Shunquan Tan, Bin Li, and Jiwu Huang. Automatic steganographic distortion  
 450 learning using a generative adversarial network. *IEEE Signal Processing Letters*, 2017.
- 451 [58] Piyu Tsai, Yu-Chen Hu, and Hsiu-Lien Yeh. Reversible image hiding scheme using predictive  
 452 coding and histogram shifting. *Signal Processing*, 2009.

- 453 [59] Clement Fuji Tsang and Jessica Fridrich. Steganalyzing images of arbitrary size with cnns.  
454     *Electronic Imaging*, 2018(7):121–1, 2018.
- 455 [60] Xintao Wang, Liangbin Xie, Chao Dong, and Ying Shan. Real-esrgan: Training real-world  
456     blind super-resolution with pure synthetic data. In *Proceedings of the IEEE/CVF International  
457     Conference on Computer Vision*, pages 1905–1914, 2021.
- 458 [61] Yinhuai Wang, Jiwen Yu, Runyi Yu, and Jian Zhang. Unlimited-size diffusion restoration. *arXiv  
459     preprint arXiv:2303.00354*, 2023.
- 460 [62] Yinhuai Wang, Jiwen Yu, and Jian Zhang. Zero-shot image restoration using denoising diffusion  
461     null-space model. In *International Conference on Learning Representations*, 2023.
- 462 [63] Zhixin Wang, Xiaoyun Zhang, Ziying Zhang, Huangjie Zheng, Mingyuan Zhou, Ya Zhang, and  
463     Yanfeng Wang. Dr2: Diffusion-based robust degradation remover for blind face restoration.  
464     2023.
- 465 [64] Mingqing Xiao, Shuxin Zheng, Chang Liu, Yaolong Wang, Di He, Guolin Ke, Jiang Bian,  
466     Zhouchen Lin, and Tie-Yan Liu. Invertible image rescaling. In *ECCV*, 2020.
- 467 [65] Guanshuo Xu, Han-Zhou Wu, and Yun-Qing Shi. Structural design of convolutional neural  
468     networks for steganalysis. *IEEE Signal Processing Letters*, 23(5):708–712, 2016.
- 469 [66] Youmin Xu, Chong Mou, Yujie Hu, Jingfen Xie, and Jian Zhang. Robust invertible image  
470     steganography. In *Proceedings of the IEEE/CVF Conference on Computer Vision and Pattern  
471     Recognition*, pages 7875–7884, 2022.
- 472 [67] Jianhua Yang, Danyang Ruan, Jiwu Huang, Xiangui Kang, and Yun-Qing Shi. An embedding  
473     cost learning framework using gan. *TIFS*, 2019.
- 474 [68] Mehdi Yedroudj, Frédéric Comby, and Marc Chaumont. Yedroudj-net: An efficient cnn for  
475     spatial steganalysis. In *2018 IEEE International Conference on Acoustics, Speech and Signal  
476     Processing (ICASSP)*, pages 2092–2096. IEEE, 2018.
- 477 [69] Weike You, Hong Zhang, and Xianfeng Zhao. A siamese cnn for image steganalysis. *IEEE  
478     Transactions on Information Forensics and Security*, 16:291–306, 2020.
- 479 [70] Jiwen Yu, Yinhuai Wang, Chen Zhao, Bernard Ghanem, and Jian Zhang. Freedom: Training-free  
480     energy-guided conditional diffusion model. *arXiv:2303.09833*, 2023.
- 481 [71] Kevin Alex Zhang, Alfredo Cuesta-Infante, Lei Xu, and Kalyan Veeramachaneni. Steganogan:  
482     High capacity image steganography with gans. *arXiv preprint arXiv:1901.03892*, 2019.
- 483 [72] Lvmin Zhang and Maneesh Agrawala. Adding conditional control to text-to-image diffusion  
484     models. *arXiv preprint arXiv:2302.05543*, 2023.
- 485 [73] Min Zhao, Fan Bao, Chongxuan Li, and Jun Zhu. Eggsde: Unpaired image-to-image translation  
486     via energy-guided stochastic differential equations. *Advances in Neural Information Processing  
487     Systems (NeurIPS)*, 2022.
- 488 [74] Zhili Zhou, Huiyu Sun, Rohan Harit, Xianyi Chen, and Xingming Sun. Coverless image  
489     steganography without embedding. In *Cloud Computing and Security: First International  
490     Conference, ICCCCS 2015, Nanjing, China, August 13–15, 2015. Revised Selected Papers 1*,  
491     pages 123–132. Springer, 2015.
- 492 [75] Jiren Zhu, Russell Kaplan, Justin Johnson, and Li Fei-Fei. Hidden: Hiding data with deep  
493     networks. In *ECCV*, 2018.
- 494 [76] Jun-Yan Zhu, Taesung Park, Phillip Isola, and Alexei A Efros. Unpaired image-to-image  
495     translation using cycle-consistent adversarial networks. In *Proceedings of the IEEE international  
496     conference on computer vision*, pages 2223–2232, 2017.